EXPERIMENTAL STUDY OF TEMPERATURE INVERSIONS ABOVE URBAN AREA USING UNMANNED AERIAL VEHICLE

by

Adnan MAŠIĆ*, Dževad BIBIĆ, Boran PIKULA, Emina DŽAFEROVIĆ-MAŠIĆ, and Rajfa MUSEMIĆ

Faculty of Mechanical Engineering, University of Sarajevo, Sarajevo, Bosnia and Herzegovina

Original scientific paper
https://doi.org/10.2298/TSCI180227250M

Vertical temperature profiles represent a very important factor for various analytical and numerical studies, such as weather forecasts, air pollution models and CFD simulations. These temperature profiles are especially important during the winter periods, when temperature inversions occur. The cities in the natural valleys, such as the city of Sarajevo, B&H, are strongly affected by this phenomenon. In this paper, a method for quantitative characterization of vertical temperature profiles, which is based on the in-house developed data acquisition system and the unmanned aerial vehicle, is presented. Comprehensive calibration and verification procedure was performed and explained in details. Field measurements were focused on the winter period and extreme temperature inversion scenarios. The correlation with the air pollution in the city, for the same period, was discussed as well.

Key words: *temperature inversion, unmanned aerial vehicle, data acquisition system, air pollution, Sarajevo*

Introduction

Temperature inversion is a natural phenomenon which occurs often in the winter period: layer of air where temperature increases with height is formed at some altitude above the ground. Natural convection is prevented through the inversion layer, which acts as the lid above the area. If the temperature inversion appears above the urban area, it is usually associated with increased air pollution below the inversion layer. The temperature inversion may last for few hours or sometimes much longer. The height above the ground where inversion layer starts and temperature gradient within inversion layer are two primary quantitative characteristics of the temperature inversion. These quantitative characteristics are important due to several reasons:

– strong inversions appear over cities in the natural valleys, which lead to the dramatic increase of air pollution in such cities,
– reliable data for vertical temperature profiles can be used to predict expected episodes of strong air pollution before pollutants concentrations reach extreme values, and
– vertical temperature profiles are required input for computer programs with models of air dispersion, and simulations in the framework of CFD.

The city of Sarajevo is situated in the natural valley, with relatively harsh climate during the winter. Prior to this study, there were no data available about temperature profiles in

* Corresponding author, e-mail: masic@mef.unsa.ba

typical winter scenarios in Sarajevo. The governmental institutions do not perform measurements of vertical profiles in our country, due to high costs (of traditional methods). The aim of this study is twofold:

– to obtain reliable data for vertical temperature profiles above the city of Sarajevo and
– to demonstrate and evaluate a novel, innovative, approach for low-cost vertical sampling which is accurate and reliable.

Several techniques were considered. The weather balloon with radiosonde was obvious candidate, but due to some limitations [1] and associated costs – it was rejected. An interesting possibility was to use the instrument which measures the microwave radiation at different elevation angles [2], but it was not available and the accuracy of such approach was questionable. The decent option is the network of ground-based automatic weather stations, such as the one presented in [3]. However, it requires significant construction work to build such a network and, strictly speaking, it does not provide vertical profiles, since the individual stations are horizontally displaced (an assumption that the field temperature is horizontally homogeneous in winter period is used). Alternatively, the ropeway could be used for in-situ measurements [4] (there is the same problem with the assumption of horizontal homogeneity of the temperature field). Comprehensive studies that use satellite sensing in combination with numerical simulations [5] and ground-based observations [6] recently appeared.

Finally, the method based on the unmanned aerial vehicle (UAV) was chosen, due to several advantages:

– lower costs (contrary to the weather balloon, UAV can be used many times, making the total cost per single measurement much lower),
– deployment possible anywhere (required landing area is comparable to the car's parking place),
– great vertical alignment and ability to control all flight parameters (including autonomous and repeatable flight paths), and
– possibility to measure the temperature profile in both directions (ascending and descending), *etc.*

The project started in 2014, with the initial evaluation of the concept and first prototype of both data acquisition system (DAS) and small UAV with four motors, taking off for the first time in early 2015 [7]. Various sensors and flight parameters were tested. Evaluation of the prototypes resulted in the decision that all systems should be developed in-house if possible, and for those components where this is not the case (flight controller for example) open-source solutions are preferred over the commercial (closed-source) products. In that way, full control of all DAS and UAV parameters is available at all times.

In the meantime, some other groups reported their attempts to use UAV for measurements of: environmental variables in greenhouses [8], air pollution [9], meteorological variables and methane [10], and air sampling on Ascension Island [11]. Fixed-wing, commercially available UAV and sensors were used to measure vertical temperature profiles in [12, 13]. These are not suitable for urban environment (aircrafts require space for landing) and do not perform vertical flights.

The apparatus

Main components of our system are DAS and UAV. The simplified schematics of the DAS is presented in the fig. 1. The temperature sensing element is a thermistor with the negative temperature coefficient (NTC). It has the small thermal capacity (thus, fast response to the changes of ambient temperature), small dimensions (0.8 mm in diameter) and very good mechanical properties (it is encapsulated in glass).

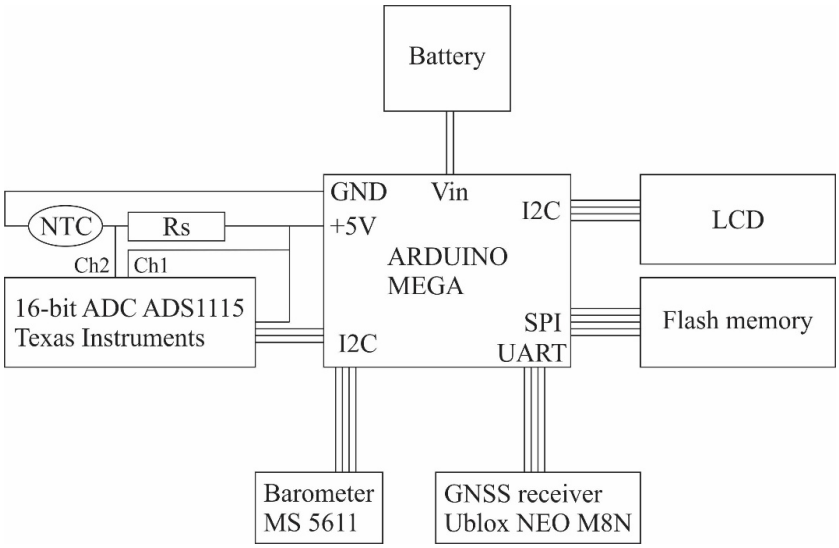

Figure 1. Simplified block-diagram of the DAS

The reference voltage of 5 V was applied to the NTC over the serial resistor, Rs, which was chosen in such a way that the self-heating effect was eliminated (an order of magnitude below the sensor's uncertainty). Analog to digital converter (ADC) is Texas Instruments ADS1115 (16-bit), which offers 0.1875 mV resolution in the interval from –6.144 V to +6.144 V. Two channels (out of four) of ADS1115 are used for temperature readings: one permanently monitors the 5 V voltage reference, the other samples the voltage across the NTC (as shown in the fig. 1). The ADC has I2C bus interface, and an Arduino Mega was used as the host microcontroller. Apart from temperature, the DAS is equipped with GNSS receiver (Ublox 8th generation, with the concurrent reception of signals from GPS and GLONASS satellites), barometer, LCD display and card memory slot. Regarding the interfaces, the LCD and barometer are I2C devices, the flash memory interface is SPI, while the GNSS receiver sends NMEA (National Marine Electronics Association) sentences over the serial interface.

The UAV has evolved dramatically from the first prototype described in [7]. Now it has six motors on the frame which is our modification of commercially available carbon fiber frame. CAD model was created in SolidWorks®, and various parameters were modified and optimized in this process. Finally, the wheelbase of 710 mm was chosen (fig. 2 shows the actual frame, its CAD model and mounted DAS). The propulsion system is commercially available DJI E800, the

Figure 2. Hexacopter chassis (a), its CAD model (b) and the DAS atop (c)

flight controller is open-source Pixhawk with Arducopter software and many smaller parts are designed in-house and printed on a 3-D printer. Radio control system works in 433 MHz bands. There is also a video downlink which streams the video from two onboard cameras.

Calibration and verification

For highly accurate and reliable measurements of temperature using thermistors, it is necessary to perform the calibration of the thermistor. We have addressed this step very carefully. The calibration of the thermistor was performed at the Institute of Metrology of Bosnia and Herzegovina, using the following cutting-edge equipment, fig. 3:

– Isotech parallel tube liquid bath 915.
– Isotech 670SQ SPRT temperature sensor.
– Isotech F900 precision thermometry bridge.
– Tektronix Keithley 2000 digital multimeter.

Figure 3. The equipment used for the calibration of the thermistor

The calibration interval was from –20 °C to +40 °C, with six calibration points: –20, –10, 0, 10, 25, and 40 °C. The uncertainty of the reference thermometer was only 2 mK, and taking into account all the factors (reference thermometer, bath, bridge, unit under test, self-heating, hysteresis and repeatability), the total uncertainty of this calibration procedure is estimated to be below 20 mK in the entire interval (that is a conservative estimate). The thermistor's calibration points were shown in the fig. 4, together with the chosen interpolation method, the Steinhart-Hart equation [14]:

$$\frac{1}{T} = a + b\ln\left(R\right) + c\ln\left(R\right)^3 \tag{1}$$

The coefficients a, b, and c were calculated using the least squares regression. We can see from fig. 4 that the state of the art technology used in the calibration process, translated into a perfect fit on the graph. Of course, the right choice of the analytical curve is important as well, and the Steinhart-Hart eq. (1) is well known and recommended interpolation curve for the NTC thermistors. This is a very important step, since the NTC thermistor has non-linear characteristic (which is clearly illustrated in fig. 4. The non-linear nature of NTC curve can be represented analytically, if we calculate the first derivation of temperature in eq. (1):

$$\frac{\mathrm{d}T}{\mathrm{d}R} = -\frac{b + 3c\,\ln(R)^2}{R\left[a + b\ln(R) + c\ln(R)^3\right]^2} \quad (2)$$

Alternatively, the polynomial fit of the fifth order could be used as well, or similar approach proposed in [15].

Together with the NTC thermistor, we have calibrated the serial resistor, Rs, as well. Its temperature dependence in the selected interval is linear, and the value of its resistance changed no more than 6.8% when going from –20 °C to +40 °C.

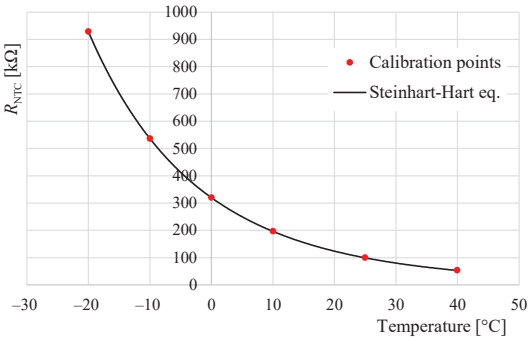

Figure 4. Calibration points and the interpolation curve

After the calibration in the laboratory, the DAS was mounted on the UAV. Computational fluid dynamics simulations, such as [8], clearly show that the optimal position of the DAS is above the rotors, where the air speed is much smaller (than below the rotors). Despite the fact that our DAS was mounted in an optimal position (considering the technical limitations), another experiment was performed: second DAS was prepared and tied to the UAV with 20 m long thread. The aim of the experiment was to check if there is any significant influence of the propellers on measured values of temperature. The thread length of 20 m was long enough to keep the bottom DAS free of turbulence created by propellers (we have verified that experimentally). At the same time, the chosen length didn't induce any significant difference of temperatures between two sensors (under test conditions, 20 m difference in height corresponds to 0.1 °C difference in temperature). Thus, two sensors are expected to produce a very good agreement.

The typical vertical mission was executed, with maximum altitude (of UAV and top DAS) of 520 m above the ground level (AGL). The results of the experiment are shown in fig. 5. We can see from the graph in fig. 5 that two sensors show very similar results, which means that the influence of the rotors on the primary DAS is not significant.

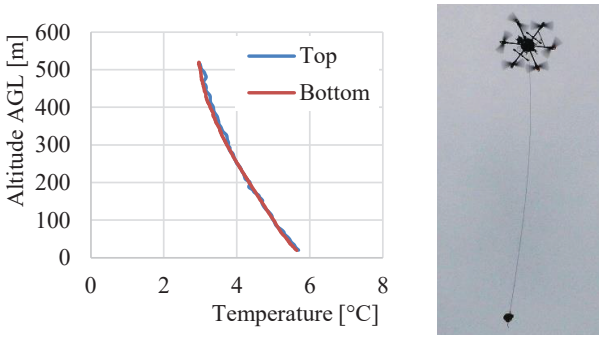

Figure 5. Test of the influence of propellers

Finally, despite the fact that the thermistor quickly reacts to the changes of ambient temperature, its time constant cannot be neglected. The UAV typically flies with vertical speed 2-3 m/s, and some hysteresis is expected, if we measure the temperature in both directions (ascending and descending). Figure 6 shows the hysteresis during the typical flight. This effect cannot be avoided, but there is an excellent opportunity for correction when using UAV: both the ascending, T_A, and descending, T_D, temperature can be used, and the arithmetic mean, T_{AVG}, is calculated, for each altitude point:

$$T_{AVG} = \frac{T_A + T_D}{2}. \quad (2)$$

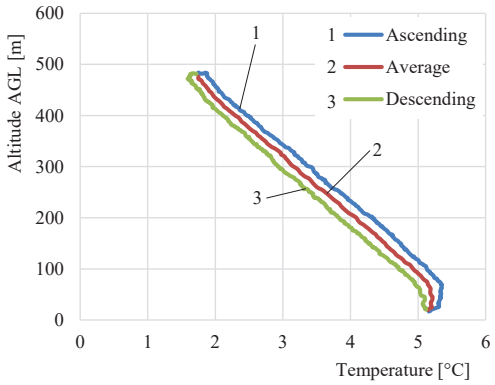

Figure 6. Continuous temperature measurement with UAV during the ascending and descending phase of flight

The graph in fig. 6 shows this correction: the temperature is measured continuously during the ascending and the descending phase of the flight, and the eq. (2) is used to estimate actual temperature. This methodology is applied to all measurements in this study.

Taking into account results of the calibration (uncertainty below 0.02 °C), test of rotor's influence (estimated below 0.20 °C) and the uncertainty due to the thermal time constant of the sensor (estimated below 0.25 °C), we can claim that all results in this study have the uncertainty of 0.5 °C or less.

The altitude AGL was calculated from the barometric formula; barometer was used for measurements of air pressure (temperature correction was implemented). Regarding the uncertainty of altitude, the greatest contribution comes from the possibility that local air presse changes during the flight, which leads to the incorrect calculation of altitude. However, typical flight time is only about 10 minutes, and it is very unlikely that the local air pressure is going to change dramatically during such a short time interval. In reality, no altitude drifts greater than 10 m were ever observed during this research. Altitude is measured using GNSS as well, but GNSS is relatively accurate for determination of horizontal position, which is not the case for the vertical position. Thus, the barometer is used for altitude calculations, with great accuracy and stability.

Results and discussion

A field campaign was performed in Sarajevo, during the winter 2016/2017, at location 43°53' 37"N, 18°22'31"E with an elevation of 557 m above sea level (denoted as L1 on pictures). Both ascending speed and descending speed are indicated in every figure. Local time and date were stamped as well. We will present 18 characteristic temperature profiles, which cover all scenarios that we have observed during the campaign. Flights are performed up to 1 km above ground level (1.5 km above sea level). Ambient temperatures occasionally went below –20 °C. Figure 7 illustrates the typical view from the UAV.

An overview of all flights is given in the tab. 1.

Figure 7. View from the UAV's main camera during the measurement

Table 1. Summary of all measurements

No.	Flight time	Observed temperature profile
1	25.12.2016, 11:40	Very strong inversion starts from 156 m AGL
2	25.12.2016, 14:40	Very strong inversion starts from 118 m AGL
3	26.12.2016, 10:20	Very strong inversion starts from 126 m AGL
4	27.12.2016, 15:20	No inversion observed
5	07.01.2017, 09:50	No inversion observed
6	11.01.2017, 11:00	No inversion observed
7	12.01.2017, 16:30	Inversion develops before sunset
8	15.01.2017, 11:40	Strong inversion layer starts from 390 m AGL
9	15.01.2017, 16:10	No inversion observed
10	22.01.2017, 10:20	Strong inversion layer starts from 316 m AGL
11	24.01.2017, 09:20	Strong inversion layer starts from 132 m AGL
12	25.01.2017, 08:20	No inversion observed
13	28.01.2017, 10:40	Mild inversion starts from 113 m AGL
14	29.01.2017, 10:20	Strong inversion starts from 47 m AGL
15	29.01.2017, 16:30	Inversion develops before sunset, mild inversion layer starts from 424 m AGL
16	31.01.2017, 17:20	Inversion develops before sunset
17	12.02.2017, 09:30	Strong inversion starts at 612 m AGL
18	15.02.2017, 11:30	Strong inversion starts from 469 m AGL

Graphs 1-3 (as described in tab. 1) show strong temperature inversions which are formed very close to the ground (the worst combination); the inversion layer starts at about 150 m above the ground and has temperature gradients in the inversion layer up to 33.5 K/km (on graph 1). This is very strong temperature inversion, and it has dramatic effects; inversions with gradients stronger than 5 K/km are known to produce severe effects on local air pollution [3]. Graphs 4-6 occasionally show very cold air, but without temperature inversion. In fig. 9, we have different scenarios. Graph 7 shows the development of inversion before sunset (due to the cold ground), with no temperature inversion in the air above 100 m AGL. Graphs 8 and 10 show temperature inversion with an interesting 'Z' profile (such profiles are discussed in [16]): inversion exists higher above the ground, and the temperature gradient is typically between 5 and 10 K/km in the inversion layer. Graphs 9 and 12 do not show inversion, while Graph 11 indicates low inversion layer height (132 m) with the gradient of about 7.9 K/km. Graphs 13-15 again show low inversion layer height with different gradients: 4.9, 10.9, and 0.2 K/km. There is again the effect of the cold ground with no inversion above 100 m AGL in Graph 16, while Graphs 17 and 18 show strong inversions that are formed higher (500 m or more) above the ground.

Figure 11 shows daily average concentrations of PM10 (particulate matter, particles smaller than 10 mm in diameter) suspended in the air, measured by the nearest governmental monitor, the Federal Hydrometeorological Institute B&H. The PM10 concentrations were measured by the beta-attenuation monitor Verewa F701 at Bjelave, Sarajevo, some 4.7 km from L1. On the secondary y-axis we have plotted reciprocal value of the inversion layer height, $1/h$ for all 18 available measurements, tab. 1. Points where inversion layer is close to the ground are appearing high on the secondary y-axis, while points without inversion sit on the horizontal axis ($1/h = 0$ for such points). From fig. 11, we can clearly see the correlation between excessive air pollution and strong temperature inversion: whenever inversion layer exists at low altitudes above the ground, high PM10 concentrations are recorded. Furthermore, when the inversion in the boundary layer breaks up, PM10 concentrations drop significantly. Some observed values

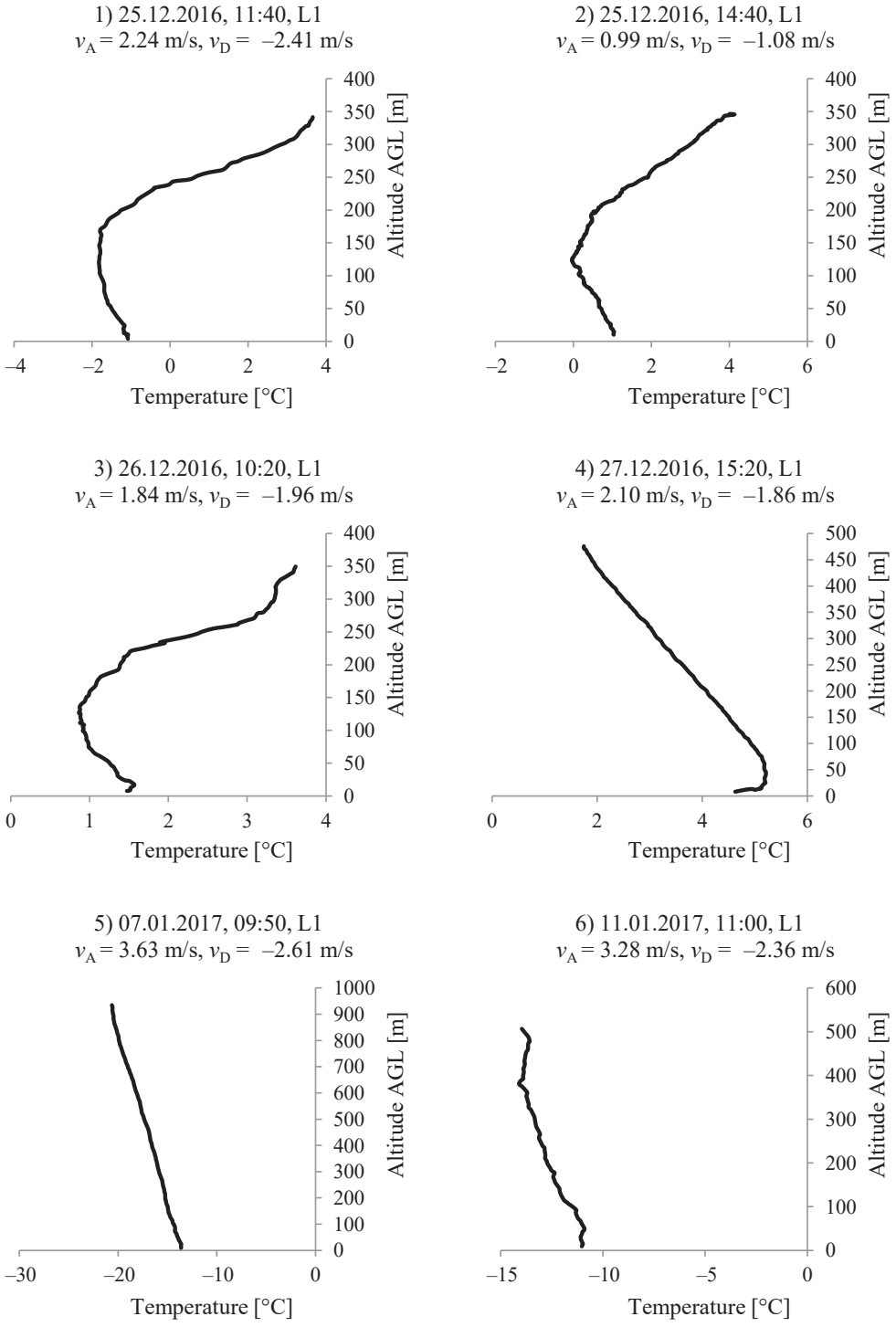

Figure 8. Temperature profiles

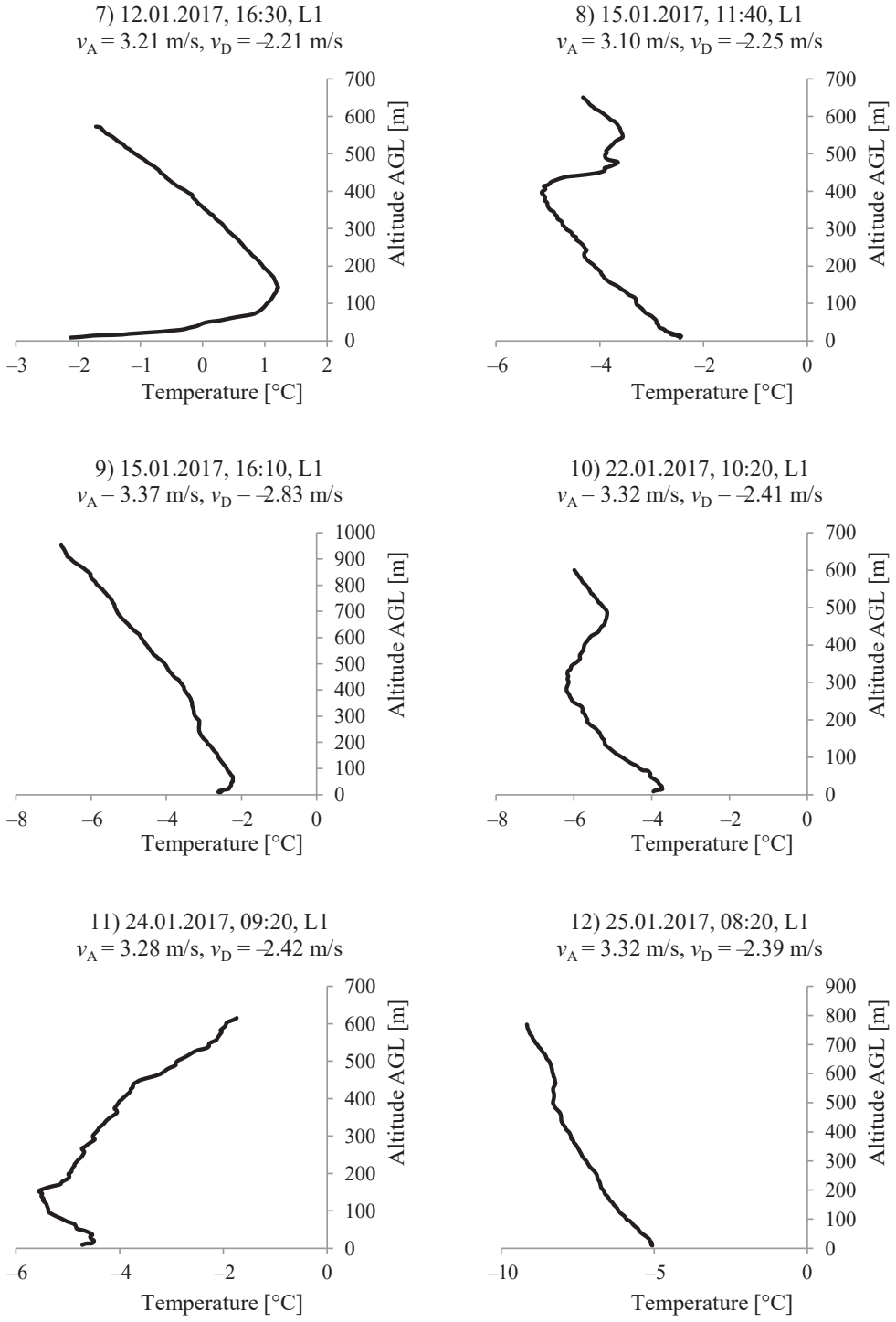

Figure 9. Temperature profiles

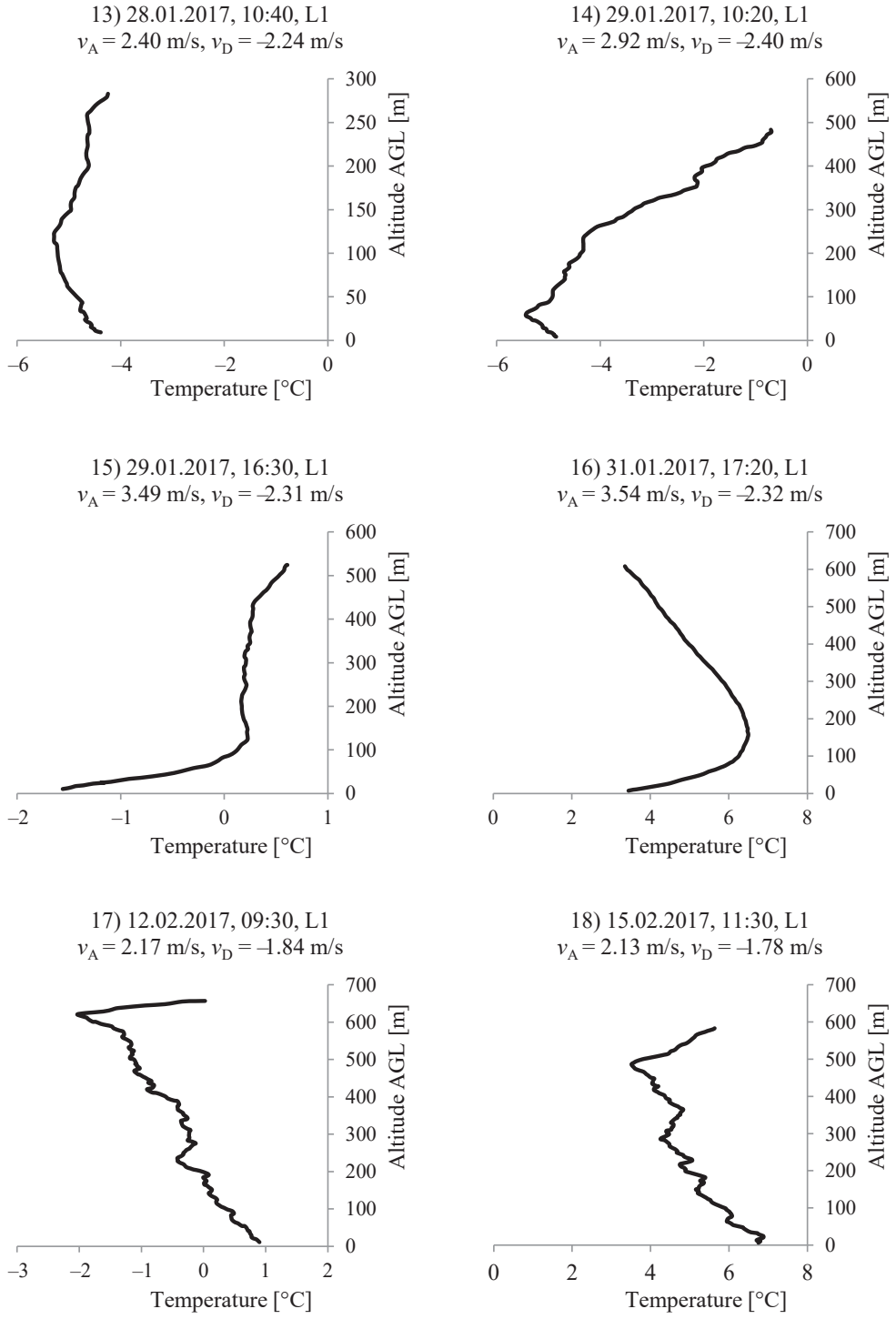

Figure 10. Temperature profiles

of PM10 concentrations (up to 600 mg/m^3) are 12 times greater than limit of 50 mg/m^3, recommended by the World Health Organization and adopted from many governmental institutions. Such level of air pollution represents major risk for the health of humans.

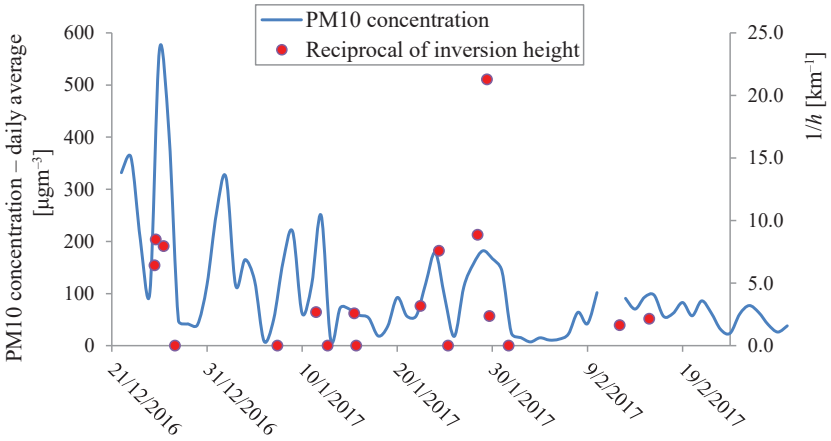

Figure 11. Correlation of PM10 air pollution and (reciprocal value of) inversion layer height

Conclusions

A comprehensive method for measurements of vertical temperature profiles using unmanned aerial vehicles is developed. Calibration and validation of all elements and procedures used for measurements were performed with great attention to all possible sources of uncertainties. A field campaign was organized during the winter 2016/2017 in Sarajevo. Various scenarios of temperature inversions were measured and analyzed. The collected data indicate unfavorable conditions: the temperature inversions were strong and shallow; with gradients in the inversion layer exceeding 30 K/km, and inversion layers often appearing below 150 m AGL. Episodes of strong and shallow inversion are correlated with hazardous air pollution, especially PM10 concentrations.

As a suggestion for future work, we propose more measurements during the longer periods. We will try to integrate sensors for air pollution parameters into our system and perform combined measurements of temperature profiles with profiles of various air pollutant concentrations. This will be reported in the near future, hopefully.

Acknowledgment

This work was supported by the Ministry of Education of Canton Sarajevo, No. 11-05-38-16631-8/16.

Also, it would not be at its greatest value without a considerable help of the Institute of Metrology of Bosnia and Herzegovina (IMB&H) and their excellent staff at the Laboratory for Temperature and Humidity, where the calibration of our temperature sensor was performed with the highest quality and international reference and traceability.

Nomenclature

a – coefficient of the first term in Steinhart-Hart equation

b – coefficient of the second term in Steinhart-Hart equation

c – voefficient of the third term in Steinhart-Hart equation
R – electric resistance, [W]
T – temperature, [K]
T_A – temperature readings during the ascend of the UAV, [K]
T_D – temperature readings during the descend of the UAV, [K]
v_A – vertical velocity of the UAV during the ascend, [ms^{-1}]
v_D – vertical velocity of the UAV during the descend, [ms^{-1}]

References

[1] Mahesh, A., *et al.*, Radiosonde Temperature Measurements in Strong Inversions: Correction for Thermal Lag Based on an Experiment at the South Pole, *Journal of Atmospheric and Oceanic Technology*, *14* (1997), Feb., pp. 45-53
[2] Wolf, T., *et al.*, Analysis of the Vertical Temperature Structure in the Bergen Valley, Norway, and its Connection to Pollution Episodes, *Journal of Geophysical Research: Atmospheres*, *119* (2014), 18, pp. 10645-10662
[3] Largeron, Y., Staquet C., Persistent Inversion Dynamics and Wintertime PM10 Air Pollution in Alpine Valleys, *Atmospheric Environment*, *135* (2016), June, pp. 92-108
[4] Zawadzka, O., *et al.*, Study of the Vertical Variability of Aerosol Properties Based on Cable Cars in-Situ Measurements, *Atmospheric Pollution Research*, *8* (2017), 5, pp. 968-978
[5] Wang, Q., *et al.*, A Quantitatively Operational Judging Method for the Process of Large Regional Heavy Haze Event Based on Satellite Remote Sensing and Numerical Simulations, *Atmosphere*, *8* (2017), 11, pp. 1-15
[6] Liu, B.*, et. al.*, Study of Continuous Air Pollution in Winter Over Wuhan Based on Ground-Based and Satellite Observations, *Atmospheric Pollution Research*, *9* (2018), 1, pp. 156-165
[7] Masic, A., Unmanned Aerial Vehicle as Data Acquisiton System, *Journal of Trends in the Development of Machinery and Associated Technology*, *1* (2015), Jan., pp. 181-184
[8] Roldan, J. J., *et al.*, Mini-UAV Based Sensory System for Measuring Environmental Variables in Greenhouses, *Sensors*, *15* (2015), 2, pp. 3334-3350
[9] Villa, T. F., *et al.*, Development and Validation of a UAV Based System for Air Pollution Measurements, *Sensors*, *16* (2016), 12, pp. 1-15
[10] Brosy, C., *et al.*, Simultaneous Multicopter-based Air Sampling and Sensing of Meteorological Variables, *Atmospheric Measuremetns Techniques*, *10* (2017), 8, pp. 2773–2784
[11] Greatwood, C., *et al.*, Atmospheric Sampling on Ascension Island Using Multirotor UAVs, *Sensors*, *17* (2017), 6, pp. 1-24
[12] Cassano, J. J., Observations of Atmospheric Boundary Layer Temperature Profiles with a Small Unmanned Aerial Vehicle, *Antarctic Science*, *26* (2014), 2, pp. 205-213
[13] Dias, N. L., Obtaining Potential Virtual Temperature Profiles, Entrainment Fluxes, and Spectra from Mini Unmanned Aerial Vehicle Data, *Boundary-Layer Meteorology*, *145* (2012), 1, pp. 93-111
[14] Steinhart, J. S., Hart, S. R., Calibration Curves for Thermistors, *Deep-Sea Research and Oceanographic Abstracts*, *15* (1968), 4, pp. 497-503
[15] Ilic, D., *et al.*, Temperature Measurements by Means of NTC Resistors and a Two-parameter Approximation Curve, *Measurement*, *41* (2008), 3, pp. 294-299
[16] Fochesatto, G. J., Methodology for Determining Multilayered Temperature Inversions, *Atmospheric Measuremetns Techniques*, *8* (2015), May, pp. 2051-2060

Paper submitted: February 27, 2018
Paper revised: August 13, 2018
Paper accepted: August 22, 2018